HIGH VELOCITY IMPACT EXPERIMENTS ON POROUS ICE AGGREGATES SIMULATING COMETARY NUCLEI SURFACE: MEASUREMENTS OF POST SHOCK TEMPERATURE AROUND IMPACT CRATER. H. Sasai[1], M. Yasui[1], M. Arakawa[1], and K. Shirai[1]. [1]Graduate School of Science, Kobe University (1-1, Rokkodai-cho, Nada-ku, Kobe, 6578501, Japan, 199s408s@stu.kobe-u.ac.jp).

Introduction: Recent spacecraft explorations and ground-based observations have revealed that cometary nuclei have very low density, such as they are highly porous icy bodies (e.g., the bulk density of 67P/CG is 533 kg/m^3 [1]). When a small body collides on such porous icy bodies at high velocities, the high-velocity collision deposits a large amount of heat around the crater cavity due to the strong dissipation of the impact energy associated with the rapid attenuation of shock pressure [2]. This deposited energy is called post-shock heat and it is one of the most important heat sources on porous icy bodies. The post shock heating would form a temporal water pond below the impact crater, and aqueous alteration and organic chemical reactions might be promoted in the water pool [3, 4, 5]. Particularly, the formation environment of organic matters on cometary nuclei has not been known yet, and the chemical reaction in a temporal water pond on comets caused by the impact heating is expected to be one of the possible formation environments. There are several numerical simulations related to the post-shock heat around the impact craters on icy planetesimals [e.g., 6], but laboratory experiments have not been studied yet.

In this study, we conducted high-velocity impact experiments on porous icy aggregates simulating icy planetesimals and measured post-shock temperatures directly around the impact crater. Then, we examined the effect of target porosity on the post-shock heating.

Experimental Methods:

Preparation of targets. We prepared cylindrical porous ice targets with the porosity of 40, 50, and 60% by compacting ice grains (< 710 μm) in a mold in a cold room at -15 ºC. They were sintered in a freezer (-20 ºC), for 2 days (40 and 60%) and for 2 hours to 4 months (50%). 3–5 thermocouples were embedded in the target at different distances from the impact point to measure the temperature. The acrylic plate having a small hole in the center was installed on the target surface to prevent the destruction of the target surface by spallation .

Impact experiments. We conducted impact experiments by using a two-stage light gas gun at Kobe Univ. installed in a cold room at -15°C. The aluminum sphere with the diameter of 2 mm was used as a projectile. The impact velocity (v_i) was 4.2 km/s for 40% and 60% targets and 3.0–5.8 km/s for 50% targets. We observed cratering processes by using a high-speed camera. The temperatures measured by thermocouples were recorded by a data logger for 5 minutes after the impact.

Analysis. We observed the crater morphology and determined the positions of thermocouples by cutting the target after each shot . We also measured the crater dimension and recovered fragments of refrozen ice pieces remained on the crater wall.

Results:

Crater morphology. Fig. 1a shows the photos of the impact craters taken from the top and the side; the schematic illustration of the impact crater observed from the side is shown in Fig. 1b. All impact craters had a pit beneath the small spalling area. These features are typical for the impact craters in the strength regime [7]. We also observed the refrozen layer on the wall as a black area. The thickness of the refrozen layer covering the pit wall was almost uniform, but several bumps were observed. The bumps on the pit bottom was composed of the refrozen water mixed with the initial ice grains and the disrupted fine projectile.

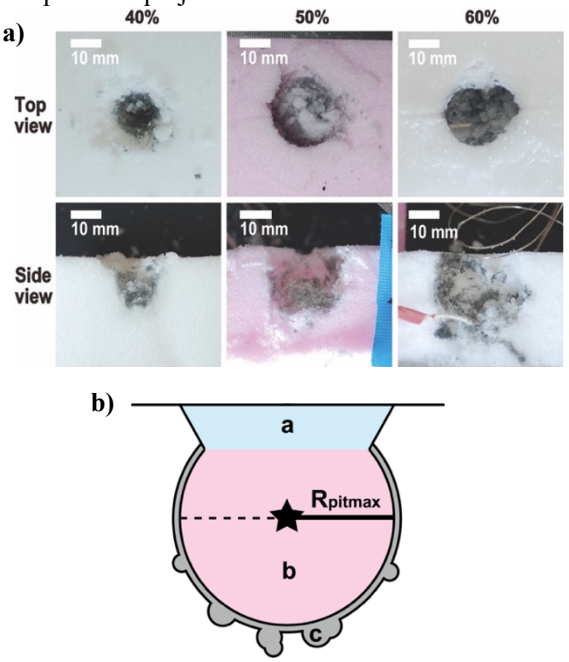

Fig. 1: a) Photographs of the impact craters. The upper photos were taken from the top and the lower were taken from the side. The v_i was 4 km/s , and the sintering duration (t_s) was 2 days. b) Schematic illustration of the crater morphology. The star symbol represents the center of the pit.

Crater size. Fig. 1 shows that the spalling diameter did not change with the target porosity while the pit

diameter increased with the increase of the target porosity. So, the maximum pit radius (R_{pitmax}) was measured by using the photos taken from the side (Fig. 1a). The R_{pitmax} is defined as shown in Fig. 1b. Furthermore, we applied our results to the crater size scaling law to compare with the previous results of non-porous crystalline ice [8]. The crater size scaling law in the strength regime was described as follows [9], $R(\rho/m)^{1/3} = H[Y/\rho v_i^2]^{-\mu/2}$, where R is the crater radius, ρ is the target density, m is the projectile mass, We measured the target compressive strength Y in this study (0.26 MPa for 40% targets, 0.076 MPa for 50%, and 0.022 MPa for 60%). The μ and H are the constants. Fig. 2 shows the relationship between the $\pi_{Rpitmax}$ ($=R(\rho/m)^{1/3}$) and the π_Y ($=Y/\rho v_i^2$). The data was scattered slightly but they were almost consistent with each other, irrespective of the porosity and the sintering duration, t_s. All data could be fitted by one power law equation and the empirical equation was obtained as $\pi_{Rpitmax} = 0.087\pi_Y^{-0.33}$. Our scaling law for porous ice showed about 5 times smaller than that for non-porous crystalline ice. This might be caused by the strong pressure decay in our porous targets [e.g., 10,11,12].

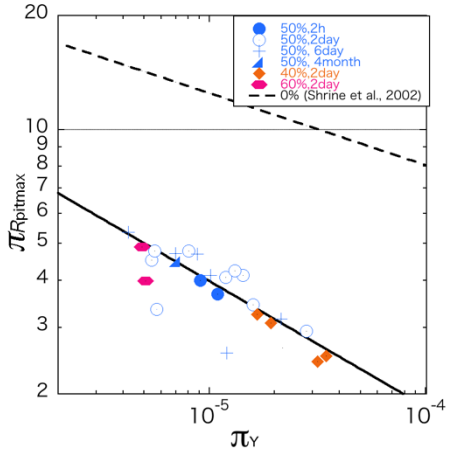

Fig. 2: Relationship between the π_Y and $\pi_{Rpitmax}$. The solid line shows the fitting line by using our all data. The dashed line shows the previous results of non-porous water ice [8].

Post-shock temperature. Fig. 3 shows the example of the temperature changes (ΔT) with time at different distances (x), where ΔT is defined as the temperature difference between the observed temperature and the initial temperature and the x is the distance between the pit center and the position of the thermocouple. The ΔT rose up rapidly after the impact and then it decreased gradually as the time passed. Furthermore, the maximum ΔT decreased with the increase of the x while the arrival time at the maximum ΔT increased with the increase of x.

Next, we studied the relationship between the maximum ΔT (ΔT_{max}) and the x as shown in Fig. 4, where

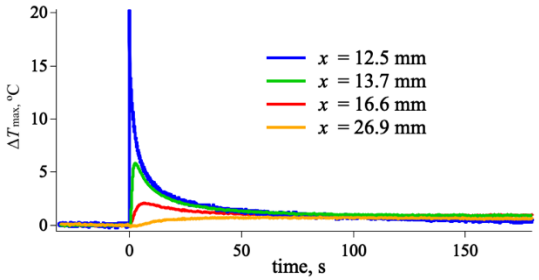

Fig. 3: Examples of the temperature change with the time. The target porosity is 60% and the impact v_i is 4 km/s. The color indicates the thermocouple positions, x.

the x was normalized by the maximum pit radius (R_{pitmax}).

The ΔT_{max} decreased exponentially with the increase of the normalized distance. Furthermore, the ΔT_{max} does not change with the target porosity. So, all data was fitted by one power law equation using normalized x, then it was obtained to be $\Delta T_{max}=7.3(x/R_{pitmax})^{-2.8}$. Additionally, the temperatures near the crater wall (that is, $x/R_{pitmax} < 1$) rose up beyond 0 ºC. This means that the ice grains near the crater wall were melted.

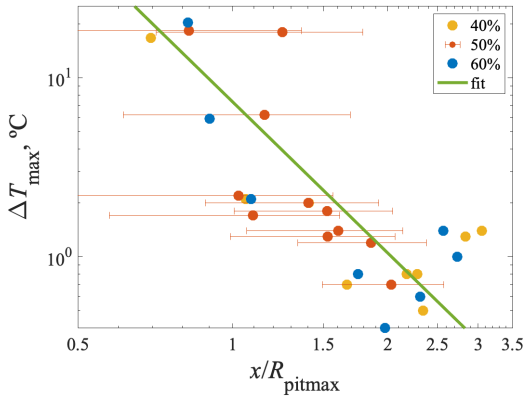

Fig. 4: Relationship between the ΔT_{max} and the normalized distance, x/R_{pitmax}. The t_s is 2 days and the v_i is 4 km/s. The error bars of 50% targets shows the measurement error of the thermocouple position.

References: [1] Pätzold et al. (2016), *Nature* 539, 63–65. [2] Housen et al. (2018) *Icarus* 163, 102–119. [3] Kebukawa & Cody (2015) *Icarus* 248, 412–423. [4] McSween et al. (2002) *Asteroids III*, 559–571. [5] Prialnik et al. (2004) *Comets II*, 359-387. [6] Kraus et al. (2011), Icarus 214, 724-738 [7] Michikami et al. (2007) *Planet. Space Sci.* 55, 70–88. [8] Shrine et al. (2002) *Icarus* 155, 475–485. [9] Housen & Holsapple (2011) *Icarus* 211, 856–875. [10] Baldwin et al. (2007) *Meteorit. Planet. Sci.* 42, 1905−1914. [11] Poelchau et al. (2014), Icarus 242, 211–224. [12] Suzuki et al. (2012) *JGR* 117, E08012.